Supporting Information

A stable and ultrafast K ion storage anode based on phase-engineered $MoSe_2$

Lei Liu,‡ Jie Xu,‡ Jinmeng Sun, Song He, Ke Wang, Yanan Chen,* Shuming Dou, Zhuzhu Du, Hongfang Du, Wei Ai* and Wei Huang*

1. Experimental Section

1.1 Materials synthesis

Typically, nitrogen and phosphorus co-doped hierarchically porous carbon (NPC) was synthesized based on our previous work.[1] For the synthesis of 1T/2H-$MoSe_2$, 30 mg NPC was added to 40 mL ethylene glycol (EG) to form a stable dispersion. Next, 218 mg $Na_2MoO_4 \cdot 2H_2O$ was dissolved in 20 mL EG under ultrasonication, which was then added to the NPC dispersion with vigorous stirring. Subsequently, a red solution prepared by 210 mg Se powder reacting with 10 mL $N_2H_4 \cdot H_2O$ was dropwised to the above-mixed solution. After vigorous stirring for 30 min, the resulting homogeneous dispersion was transferred to a 100 mL autoclave and hydrothermally reacted at 200 °C for 12 h. The as-obtained black precipitate was collected by filtration, washed with deionized water for several times, and finally dried at 80 °C in vacuum oven over night. 1T/2H-$MoSe_2$ was then obtained after a further annealing at 600 °C for 5 h under argon (heating rate: 5 °C min^{-1}). For comparison, 1T-$MoSe_2$ was prepared under similar conditions but without NPC.

1.2 Material characterizations

SEM and TEM were acquired on a Verios G4 and FEI Talos F200X TEM, respectively. XRD patterns were measured on a Bruker D8 advance diffractometer with Cu Kα radiation. XPS was tested using an Axis Supra XPS spectrometer equipped with monochromated Al Kα. Raman spectroscopy was collected using a

Horiba LabRAM Evolution spectrometer with an excitation wavelength of 532 nm. N_2 adsorption-desorption analysis was obtained on an ASAP2460 apparatus. TGA was conducted on a Netzsch STA449F3 analyzer under air.

1.3 Electrochemical measurements

The electrochemical properties were tested in half 2032 coin-type cells with metal potassium as the counter electrode and reference electrode. The electrode was prepared by mixing 80 wt% of active materials, 10 wt% of carbon black, and 10 wt% of sodium alginate in deionized water, after which the slurry was coated onto a copper foil and dried overnight at 80 °C under vacuum. Circular electrodes were punched out, and then weighed (0.7-1.0 mg on each electrode). The electrolyte is composed of 3 M KFSI dissolved in dimethyl ether. Electrochemical tests were performed on a NEWARE battery testing system and a CHI 760D electrochemical workstation in the voltage range of 0.01-3.0 V (vs. K^+/K).

2. Supplementary Figures

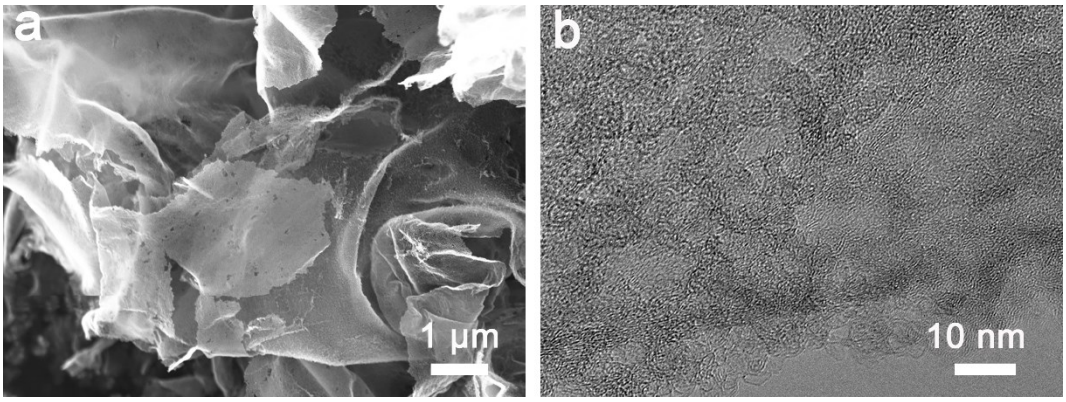

Fig. S1 (a) SEM and (b) HRTEM image of NPC.

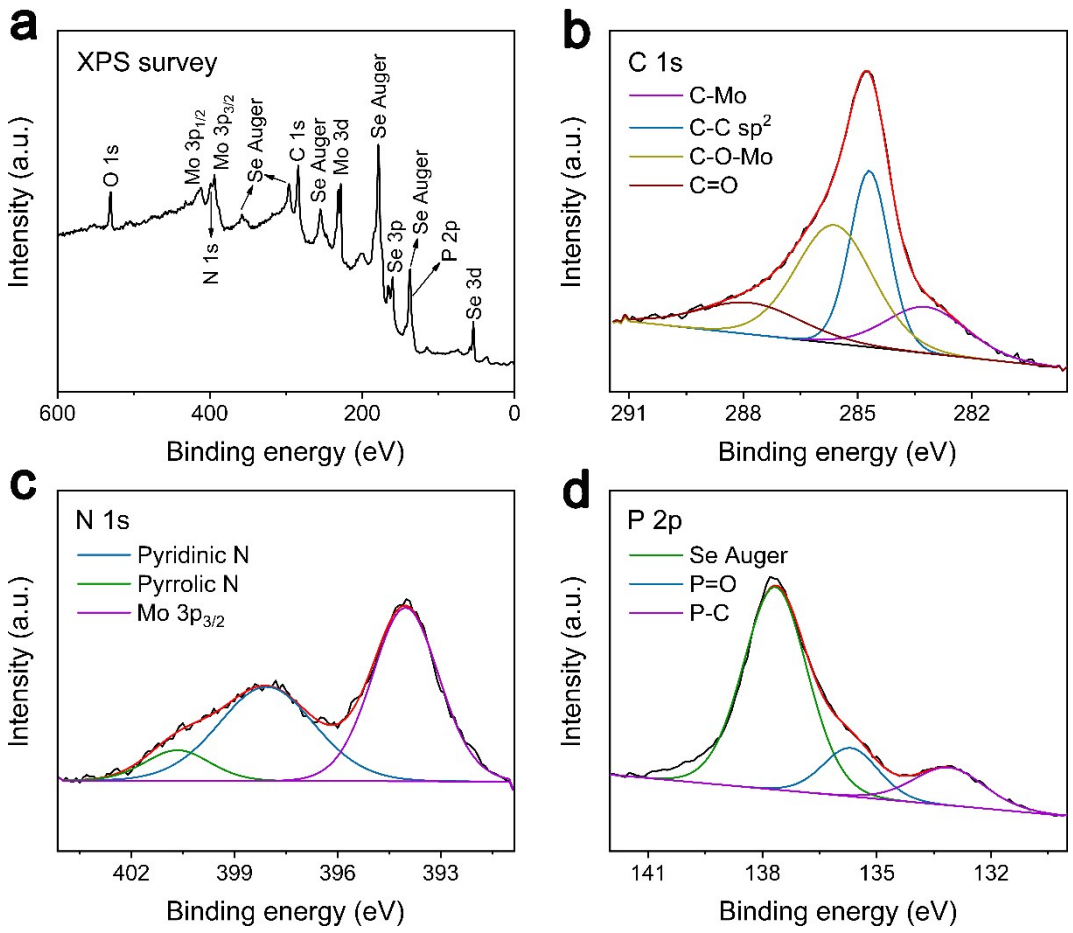

Fig. S2 (a) XPS survey, high-resolution (b) C 1s, (c) N 1s, and (d) P 2p XPS spectra of 1T/2H-$MoSe_2$.

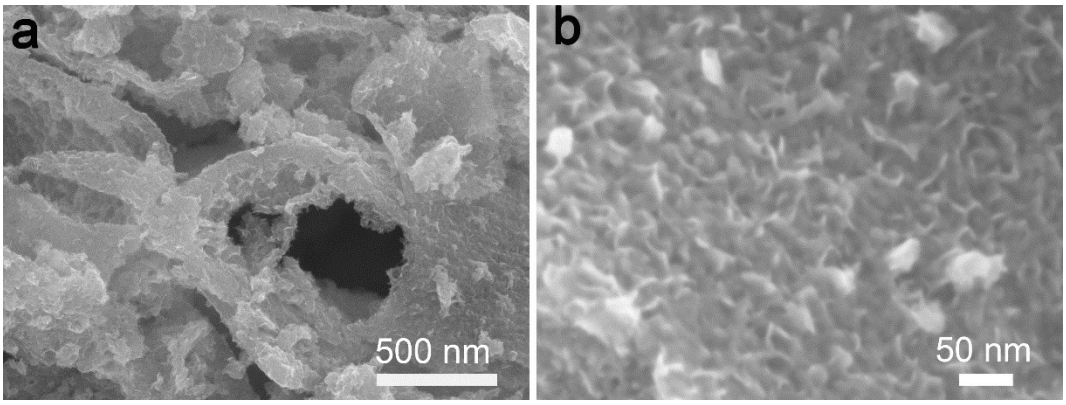

Fig. S3 (a, b) SEM images of 1T/2H-$MoSe_2$.

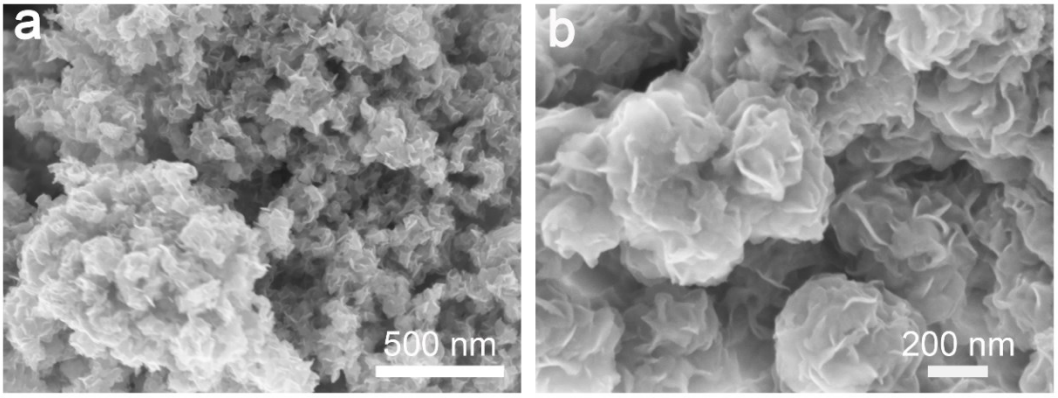

Fig. S4 (a, b) SEM images of 1T-$MoSe_2$.

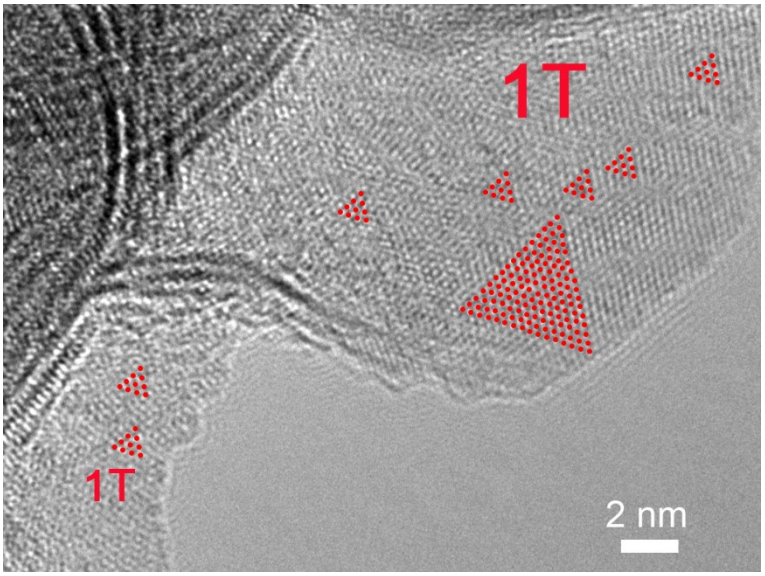

Fig. S5 HRTEM image of 1T-$MoSe_2$.

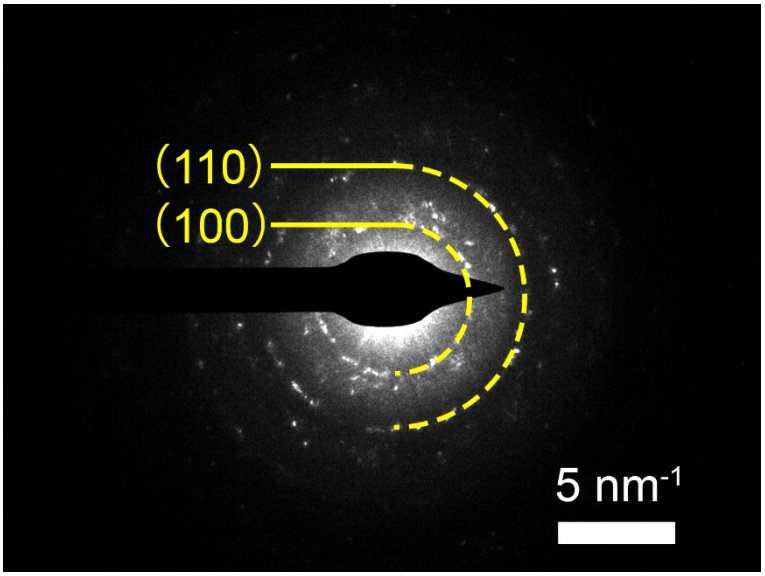

Fig. S6 SAED pattern of 1T/2H-$MoSe_2$.

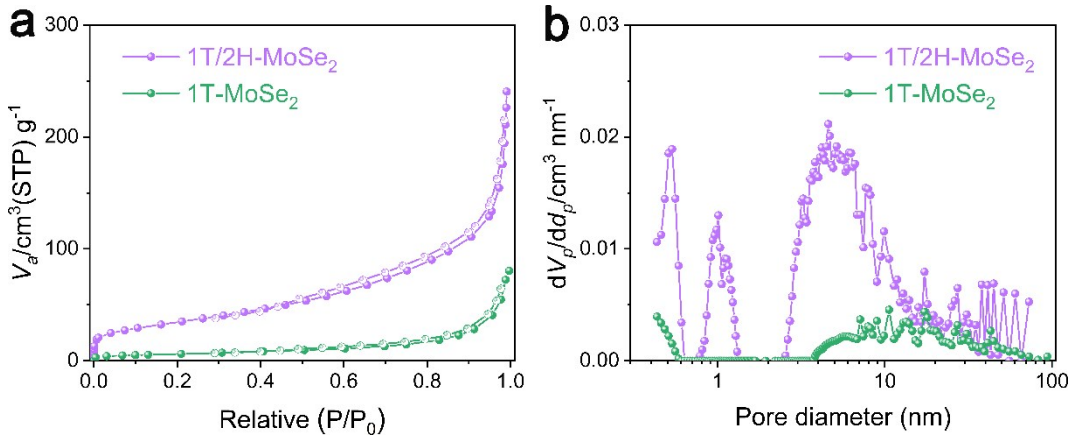

Fig. S7 (a) N_2 adsorption-desorption isotherms and (b) the corresponding NLDFT pore size distribution plots of 1T/2H-$MoSe_2$ and 1T-$MoSe_2$.

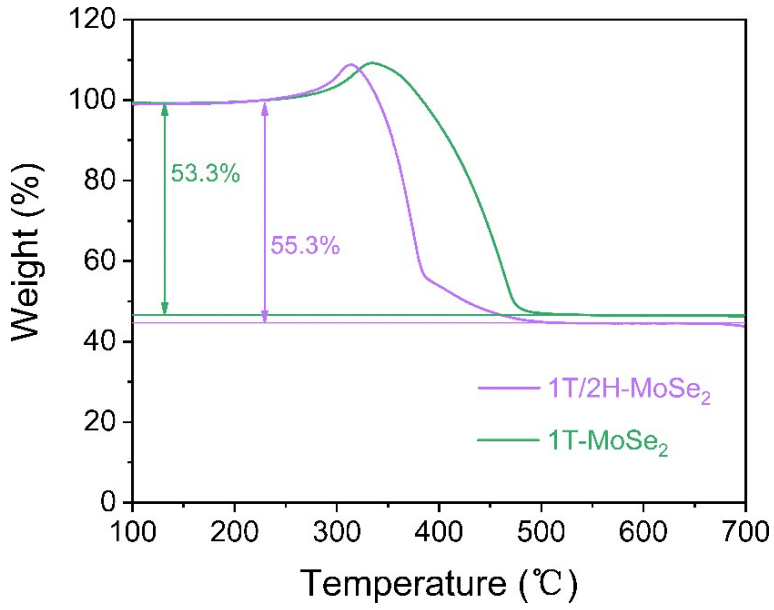

Fig. S8 TGA curves of 1T/2H-$MoSe_2$ and 1T-$MoSe_2$. In the two samples, the weight gain before 350 ℃ could be attributed to the oxidation of $MoSe_2$ to MoO_3 and SeO_2. In the case of 1T-$MoSe_2$, the weight loss resulted from the sublimation of SeO_2. In comparison, the weight loss of 1T/2H-$MoSe_2$ is equal to the sum of weight loss of $MoSe_2$ and NPC. As depicted in the formula below:[2, 3]

$A\times55.3\%=A\times Y\times53.3\%+A\times(1-Y)$

A: the mass of 1T/2H-$MoSe_2$. Y: the loading of $MoSe_2$ in the 1T/2H-$MoSe_2$. Therefore, the accurate loading of $MoSe_2$ in the 1T/2H-$MoSe_2$ is calculated to be 95.7% and the carbon content in the 1T/2H-$MoSe_2$ sample is calculated to be 4.3%.

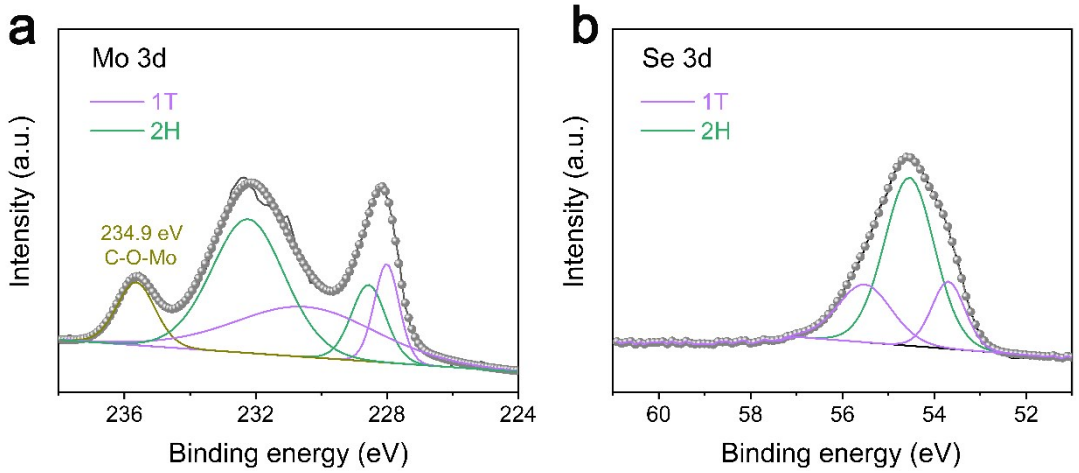

Fig. S9 High-resolution (a) Mo 3d and (b) Se 3d XPS spectra of the cycled 1T/2H-$MoSe_2$ electrode.

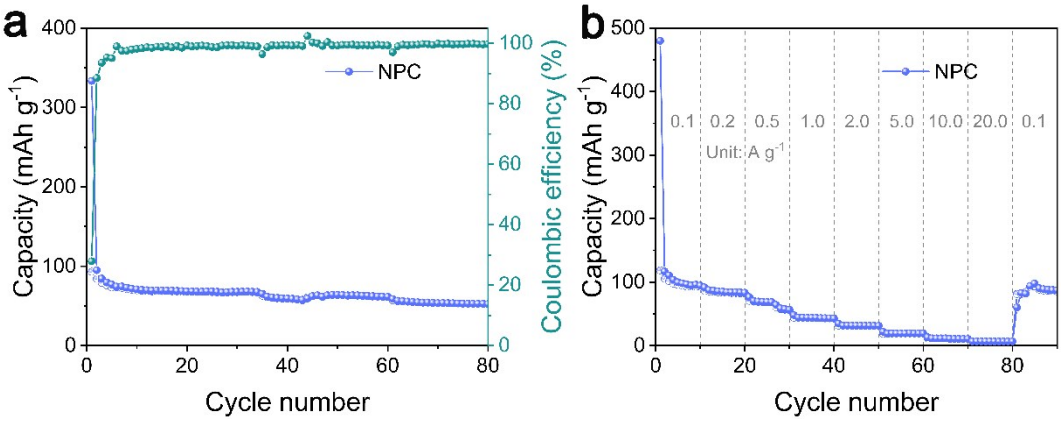

Fig. S10 (a) Cycling performance (0.2 A g^{-1}) and (b) rate capability of NPC.

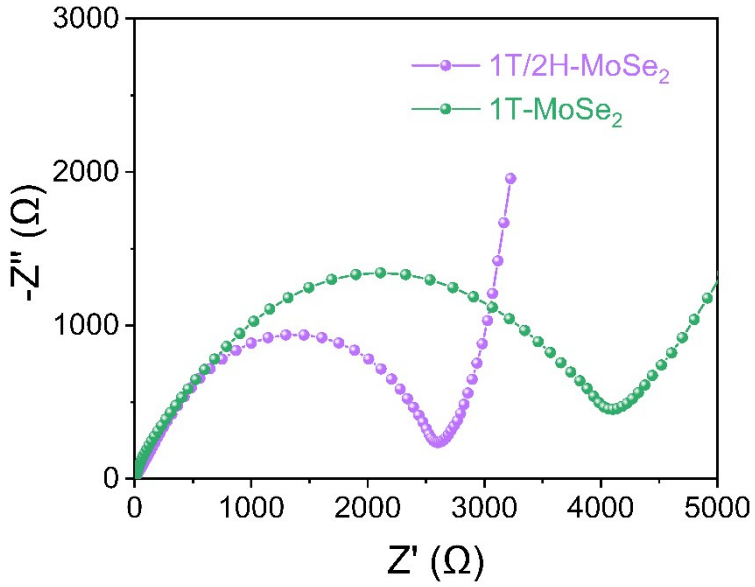

Fig. S11 Nyquist plots of the 1T/2H-$MoSe_2$ and 1T-$MoSe_2$ electrodes after 10 cycles.

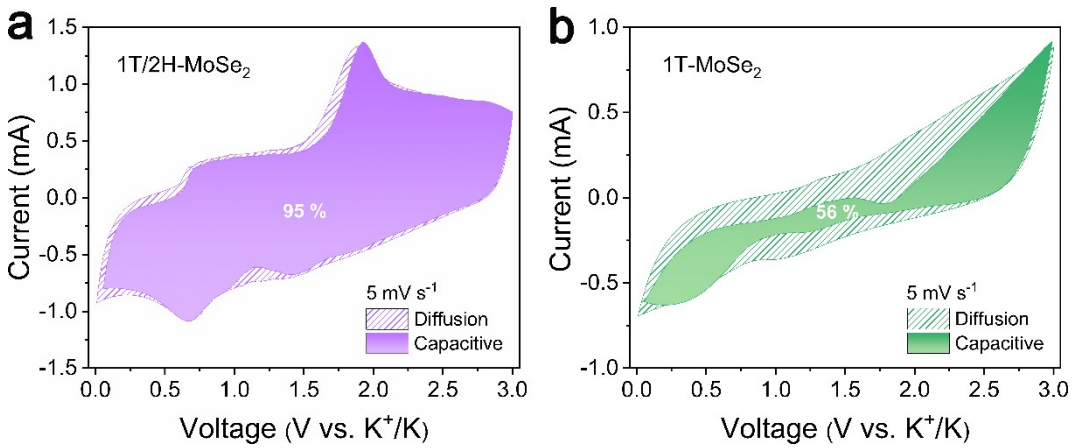

Fig. S12 The capacitive contribution to the total charge storage of (a) 1T/2H-$MoSe_2$ and (b) 1T-$MoSe_2$ electrodes at 5 mV s^{-1}.

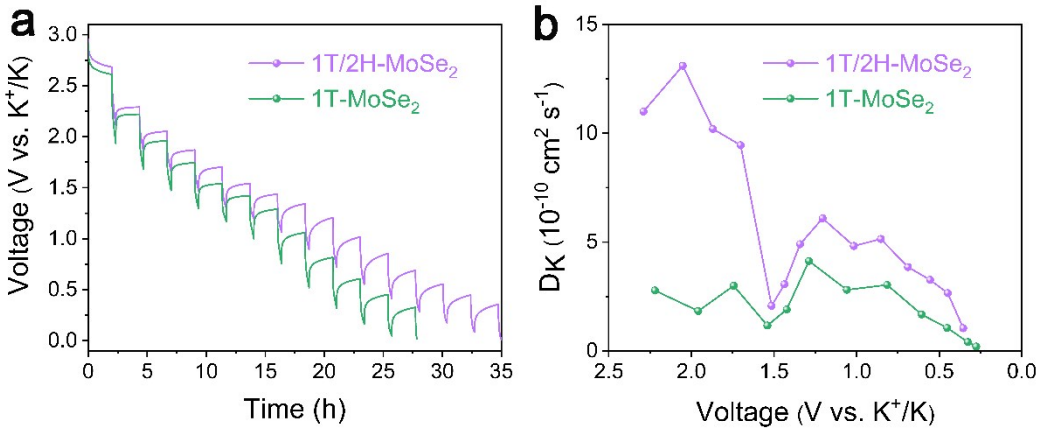

Fig. S13 (a) GITT profiles of the discharging process and (b) corresponding K ion diffusion coefficients of 1T/2H-$MoSe_2$ and 1T-$MoSe_2$.

3. Supplementary Tables

Table S1. Comparison of 1T/2H-$MoSe_2$ with the previously reported TMDs-based anodes for PIBs.

Samples	Carbon content (%)	Voltage window (V vs. K^+/K)	Rate capacity	ICE (%)	Ref
1T/2H-$MoSe_2$	**4.3**	**0.01-3.0**	**211 mAh g^{-1} at 20.0 A g^{-1}**	**61.9**	**This work**
$MoSe_2$@PNC-HNTs	36.8	0.01-3.0	79.1 mAh g^{-1} at 5.0 A g^{-1}	27.2	4
$MoSe_2$/MXene@C	—	0.01-3.0	183 mAh g^{-1} at 10.0 A g^{-1}	54.2	5
$MoSe_2$@C	—	0.1-2.5	224 mAh g^{-1} at 2.0 A g^{-1}	63.4	6
$MoSe_2$@N-C	8.2	0.01-3.0	178 mAh g^{-1} at 2.0 A g^{-1}	79.9	7
$MoSe_2$@NC	7	0.01-3.0	171 mAh g^{-1} at 5.0 A g^{-1}	60	8
N-$MoSe_2$@rGO	—	0.01-3.0	155 mAh g^{-1} at 2.0 A g^{-1}	—	9
MoS_2@HPCS	28.5	0.01-3.0	93.1 mAh g^{-1} at 2.0 A g^{-1}	37.4	10
MoS_2@NC	25	0.01-2.5	131 mAh g^{-1} at 2.0 A g^{-1}	—	11
$Co_{0.85}Se$@C	49	0.01-2.6	166 mAh g^{-1} at 5.0 A g^{-1}	50.2	12
v-MoSSe@CM	45.3	0.01-3.0	202.6 mAh g^{-1} at 5.0 A g^{-1}	53.5	13
Fe_9S_{10}@MoS_2@C	26.4	0.01-3.0	127 mAh g^{-1} at 5.0 A g^{-1}	71	14
CoSeS@C/G	7.7	0.01-3.0	195.7 mAh g^{-1} at 2.0 A g^{-1}	48	15
MoS_2@rGO	12.6	0.01-3.0	178 mAh g^{-1} at 0.5 A g^{-1}	—	16
Co_9S_8/NSC@MoS_2@NSC	—	0.01-2.6	163 mAh g^{-1} at 3.0 A g^{-1}	65.9	17
V_3S_4@C	—	0.01 - 3.0	155 mAh g^{-1} at 10.0 A g^{-1}	37	18
ZnSe@C	20.37	0.01-2.5	205 mAh g^{-1} at 0.5 A g^{-1}	47.78	19

References

1. W. Ai, X. Wang, C. Zou, Z. Du, Z. Fan, H. Zhang, P. Chen, T. Yu and W. Huang, *Small*, 2017, **13**, 1602010.
2. X. Yang, Z. Zhang, Y. Fu and Q. Li, *Nanoscale*, 2015, **7**, 10198.
3. F. Niu, J. Yang, N. Wang, D. Zhang, W. Fan, J. Yang and Y. Qian, *Adv. Funct. Mater.*, 2017, **27**, 1700522.
4. B. Li, Y. Liu, Y. Li, S. Jiao, S. Zeng, L. Shi and G. Zhang, *ACS Appl. Mater. Interfaces*, 2020, **12**, 2390.
5. H. Huang, J. Cui, G. Liu, R. Bi and L. Zhang, *ACS Nano*, 2019, **13**, 3448.
6. W. Wang, B. Jiang, C. Qian, F. Lv, J. Feng, J. Zhou, K. Wang, C. Yang, Y. Yang and S. Guo, *Adv. Mater.*, 2018, **30**, 1801812.
7. J. Ge, L. Fan, J. Wang, Q. Zhang, Z. Liu, E. Zhang, Q. Liu, X. Yu and B. Lu, *Adv. Energy Mater.*, 2018, **8**, 1801477.
8. M. Ma, S. Zhang, Y. Yao, H. Wang, H. Huang, R. Xu, J. Wang, X. Zhou, W. Yang, Z. Peng, X. Wu, Y. Hou and Y. Yu, *Adv. Mater.*, 2020, **32**, 2000958.
9. Y. Yi, Z. Sun, C. Li, Z. Tian, C. Lu, Y. Shao, J. Li, J. Sun and Z. Liu, *Adv. Funct. Mater.* , 2019, **30**, 1903878.
10. J. Hu, Y. Xie, X. Zhou and Z. Zhang, *ACS Appl. Mater. Interfaces*, 2020, **12**, 1232.
11. B. Jia, Q. Yu, Y. Zhao, M. Qin, W. Wang, Z. Liu, C. Y. Lao, Y. Liu, H. Wu, Z. Zhang and X. Qu, *Adv. Funct. Mater.*, 2018, **28**, 1803409.
12. C. Atangana Etogo, H. Huang, H. Hong, G. Liu and L. Zhang, *Energy Storage Mater.*, 2020, **24**, 167.
13. Z. Tian, N. Chui, R. Lian, Q. Yang, W. Wang, C. Yang, D. Rao, J. Huang, Y. Zhang, F. Lai, C. Liu and T. Liu, *Energy Storage Mater.*, 2020, **27**, 591.
14. C. Zhang, F. Han, F. Wang, Q. Liu, D. Zhou, F. Zhang, S. Xu, C. Fan, X. Li and J. Liu, *Energy Storage Mater.*, 2020, **24**, 208.
15. C. Wang, B. Zhang, H. Xia, L. Cao, B. Luo, X. Fan, J. Zhang and X. Ou, *Small*, 2020, **16**, 1905853.
16. K. Xie, K. Yuan, X. Li, W. Lu, C. Shen, C. Liang, R. Vajtai, P. Ajayan and B. Wei, *Small*, 2017, **13**.
17. C. Yang, J. Feng, Y. Zhang, Q. Yang, P. Li, T. Arlt, F. Lai, J. Wang, C. Yin, W. Wang, G. Qian, L. Cui, W. Yang, Y. Chen and I. Manke, *Small*, 2019, **15**, 1903720.
18. Y. Liu, Z. Sun, X. Sun, Y. Lin, K. Tan, J. Sun, L. Liang, L. Hou and C. Yuan, *Angew. Chem. Int. Ed.*, 2020, **59**, 2473.
19. J. Chu, W. Wang, Q. Yu, C. Y. Lao, L. Zhang, K. Xi, K. Han, L. Xing, L. Song, M. Wang and Y. Bao, *J. Mater. Chem. A*, 2020, **8**, 779.